RSC Advances

PAPER

View Article Online
View Journal | View Issue

Cite this: *RSC Adv.*, 2017, **7**, 5315

Magnetic damping and perpendicular magnetic anisotropy in Pd-buffered $[Co/Ni]_5$ and $[Ni/Co]_5$ multilayers

Minghong Tang,[a] Wei Li,[b] Yang Ren,[c] Zongzhi Zhang,*[a] Shitao Lou[b] and Q. Y. Jin[ab]

Received 31st October 2016
Accepted 31st December 2016

DOI: 10.1039/c6ra26087j

www.rsc.org/advances

We systematically studied the influence of Pd underlayer on the magnetic properties of perpendicular $[Co/Ni]_5$ and $[Ni/Co]_5$ multilayers by time-resolved magneto-optical Kerr effect. We found that the saturated magnetic damping constant α_0 increases continuously with increasing the Pd thickness t_{Pd}, showing no linear correlation with the perpendicular magnetic anisotropy constant K_u for both series of samples. As compared to the Co/Ni sample with the same t_{Pd}, the Ni/Co film shows lower saturation magnetization, weaker K_u but larger α_0, which can be ascribed to the presence of more paramagnetic spins at the Pd/Ni interface due to the weak exchange coupling stiffness between Ni atoms. By analyzing extrinsic damping contributions from magnetic inhomogeneities, two-magnon scattering and spin pumping effects, the intrinsic damping of perpendicular $[Ni/Co]_5$ is quantitatively determined to be 0.023. This study should provide deep understanding and effective control of magnetic damping for designing high performance magnetic memory devices.

Introduction

In recent years, magnetic multilayers or thin films with strong perpendicular magnetic anisotropy (PMA) have been widely studied due to their potential applications in spin-transfer torque magnetic random access memory (STT-MARM) and other spintronic devices.[1–4] In order to increase the STT-memory density and lower the switching energy, reducing the critical switching current density J_c is a major concern. The J_c is known to be proportional to the effective perpendicular magnetic anisotropy energy and the magnetic damping constant. And it is commonly believed that the perpendicular magnetic thin films with high K_u usually has a larger damping because of the strong spin–orbit interaction.[5] For instance, a linear relationship between intrinsic Gilbert damping constant α_0 and PMA strength has been found in some perpendicular thin films of Pt/Co/Pt sandwich, $[Co/Pd]_8$ multilayers, and $L1_0$-$FePd_{1-x}Pt_x$ ternary alloy.[6–8] However, such a correlation doesn't apply to the perpendicular Ta/CoFeB/MgO or Co/Pt multilayer systems.[9,10] The conflicting opinions, we speculate, are most probably caused by the incomprehensive consideration for various damping contributions. As we know, in addition to the intrinsic Gilbert damping resulting from spin–orbit coupling of the ferromagnetic materials, the local fluctuations of magnetization, magnetic anisotropy, as well as the magneto static fields at different sample locations would give rise to some extrinsic contributions. These extrinsic damping α_{ex} caused by inhomogeneous magnetic properties strongly relies on the surface/interface roughness and other film defects.[11,12] Moreover, at the ferromagnet (FM)/non-magnetic (NM) metal layer interface, the magnetization precession will transfer spins to the adjacent NM layers, which can also dissipate spin energy and therefore enhance the effective damping constant *via* spin-pumping effect.[13–15] In order to effectively control the magnetization switching dynamics, magnetic damping terms resulting from different origins should be carefully considered and controlled for practical applications.

Among the various perpendicular magnetic film structures, Co/Ni multilayer has attracted a great deal of interest due to its high spin polarization and low magnetic damping. Generally, a nonmagnetic underlayer with a preferred fcc (111) orientation is indispensable for achieving PMA in Co/Ni multilayers. Compared with the Cu, Au and Ti underlayer materials,[16–19] the Pd or Pt is rarely employed because incorporation of such heavy metal with strong spin–orbit coupling would introduce a large extra spin pumping term to the magnetic damping, which is undesirable since it would enhance the critical STT switching current. However, more recently, the Pd and Pt layers have gained great attentions in some new emerging spin-dependent research areas, *e.g.* current-induced spin–orbit torque (SOT) switching, which is being considered as a potential new writing method for switching a perpendicular magnetic memory bit.[20,21] A commonly used SOT device is based on a perpendicular

[a]*Key Laboratory of Micro and Nano Photonic Structures, Ministry of Education, Department of Optical Science and Engineering, Fudan University, Shanghai 200433, China. E-mail: zzzhang@fudan.edu.cn*

[b]*State Key Laboratory of Precision Spectroscopy, East China Normal University, Shanghai 200062, China*

[c]*School of Physics and Astronomy, Yunnan University, Kunming 650000, China*

multilayer stack consisting of heavy metal/ferromagnet (FM)/oxide layers, which allows for lower switching energy as compared with the conventional STT-MRAM. The SOT effect, arising from the spin–orbit coupling of the adjacent non-magnetic heavy metal layer such as Pt, Pd, Ta or W layer with a large spin Hall angle,[22–24] can generate a pure spin current to exert strong torques on the magnetic layer. In order to develop high performance SOT-MRAMs and other SOT-related devices, it will be of vital importance to carry out a systematic study on magnetization dynamics for heavy metal-buffered perpendicular magnetic thin films.

In this work, we have fabricated Pd-buffered $[Co/Ni]_5$ and $[Ni/Co]_5$ perpendicular multilayers with either Co or Ni in contact with Pd, and investigated the influences of Pd thickness and multilayer deposition sequence on the perpendicular magnetic anisotropy and magnetic damping by means of time-resolved magneto-optical Kerr effect (TR-MOKE) technique.[25] By analyzing and comparing the experimental results with those of Cu-buffered $[Ni/Co]_5$ samples, the intrinsic magnetic damping constant of Co/Ni multilayer and spin-pumping contribution from Pd underlayer are identified.

Experiments

Using a Kurt J. Lesker magnetron sputtering system, multilayer films were deposited on amorphous Corning glass substrates at room temperature (RT) under a base pressure better than 5×10^{-8} Torr. By varying the magnetic layer deposition sequence, two series of samples have been fabricated: glass/Ta(3)/Pd(t_{Pd})/$[Co(0.26)/Ni(0.6)]_5$/Ta(3) and glass/Ta(3)/Pd(t_{Pd})/$[Ni(0.6)/Co(0.26)]_5$/Ta(3) (thickness in unit of nm), where the thickness of Pd layer t_{Pd} varies from 2.5 to 40 nm. For comparison, another series of samples with a structure of glass/Ta(3)/Cu(t_{Cu})/$[Ni(0.6)/Co(0.26)]_5$/Ta(3) were also prepared, where t_{Cu} is in the range of 2.5–20 nm. The film crystallinity was checked by X-ray diffraction and atomic force microscopy. The static magnetic properties and magnetization dynamic behaviors were respectively measured by a vibrating sample magnetometer (VSM) and a TR-MOKE system.[26] The TR-MOKE measurement was performed by using a pulsed Ti:sapphire laser with a central wavelength of 800 nm, a pulse duration of 150 fs and a repetition rate of 1 kHz. A variable external magnetic field H_{ex} was applied at an angle θ_H of 65° with respect to the film normal. The respective spot diameters of pump and probe laser pulses were about 1.0 and 0.2 mm, at almost perpendicular incidence to the film plane. For better Kerr signal and negligible heating effect, in this experiment the pump and probe laser fluences were chosen as $F = 1.5$ mJ cm^{-2} and 0.07 mJ cm^{-2}, respectively.

Results and discussion

Fig. 1(a) and (b) representatively show the in-plane and out-of-plane magnetic hysteresis loops measured by VSM for the samples of Pd(5)/$[Co(0.26)/Ni(0.6)]_5$ and Pd(5)/$[Ni(0.6)/Co(0.26)]_5$. Clearly, all the samples exhibit PMA. Nevertheless, both the in-plane saturation magnetic field H_s and perpendicular coercivity H_c of $[Ni/Co]_5$ series are smaller than those of $[Co/Ni]_5$ series, implying the PMA strength is closely related to the adjacent magnetic layer material deposited on top of the Pd underlayer. In order to clearly interpret the variation trends of PMA strength, the saturation magnetization M_s and uniaxial magnetic anisotropy constant K_u are derived and plotted in Fig. 1(c) and (d) as a function of t_{Pd}. The K_u value is calculated according to the relationship of $K_u = M_s H_s/2 + 2\pi M_s^2$, where M_s is the saturation magnetization and H_s is the effective perpendicular anisotropy field obtained from the in-plane hysteresis loop. As shown in Fig. 1(c), apart from the initial enhancement arising from the induced polarization of Pd layer at $t_{Pd} \leq 5$ nm,[27] the M_s value decreases considerably with increasing the Pd layer thickness for both series of samples. We consider the reduction of M_s is due to the increased thickness of magnetically dead layer formed at the Pd/Co or Pd/Ni interface. The

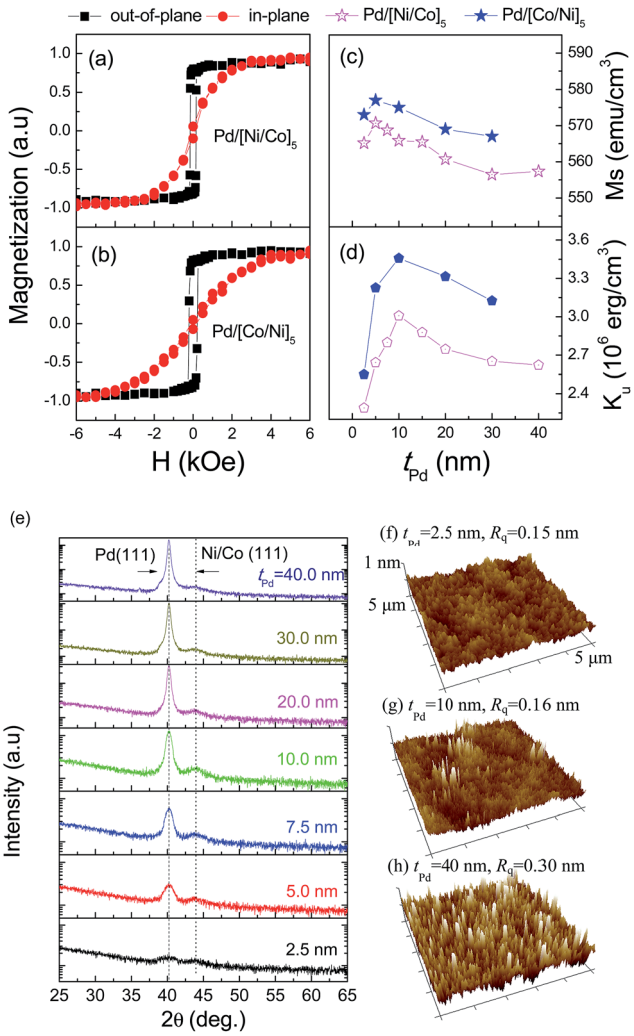

Fig. 1 The in-plane and out-of-plane magnetic hysteresis loops for samples of (a) Pd(5)/$[Ni(0.6)/Co(0.26)]_5$ and (b) Pd(5)/$[Co(0.26)/Ni(0.6)]_5$. (c) The saturation magnetization M_s and (d) the uniaxial magnetic anisotropy energy density K_u as a function of Pd underlay layer thickness t_{Pd} for the two types of samples. (e) The XRD patterns for the $[Ni(0.6)/Co(0.26)]_5$ samples with different t_{Pd}. (f)–(h) The AFM images measured on the sample surfaces of glass/Pd(t_{Pd}) with t_{Pd} = 2.5, 10 and 40 nm.

thicker Pd layer has a rougher surface,[28] and thereupon would bring a thicker dead layer in which the magnetic spins are in a disordered (paramagnetic) state possibly due to intermixing or alloy formation.[29] Fig. 1(d) shows the t_{Pd} dependence of K_u, it firstly increases and then decreases after reaching its maximum value at $t_{Pd} = 10$ nm. Such non-monotonic variation behavior comes from the competition between the roles of (111) texture and Pd surface roughness. In order to verify our interpretations, the XRD patterns for the Pd(t_{Pd})/[Ni(0.6)/Co(0.26)]$_5$ samples and the surfaces AFM images of glass/Pd(t_{Pd}) have been plotted respectively in Fig. 1(e) and (f)–(h). When t_{Pd} increases from 2.5 nm to 10 nm, the Ni/Co (111) peak enhances gradually and plays a dominant role on the initial increase of PMA strength. However, when t_{Pd} is over 10 nm, the peak intensity becomes decreasing mostly owing to the increased Pd surface roughness. As shown in Fig. 1(h), the root-mean-square roughness (R_q) of t_{Pd} = 40 nm is as large as 0.30 nm, which should be responsible for the subsequent degradation of M_s and K_u. In particular, it should be noted that for the samples with the same t_{Pd}, the Pd/[Ni/Co]$_5$ structure owns much lower M_s and K_u than the Pd/[Co/Ni]$_5$ one. This is understandable since the exchange coupling stiffness and Curie temperature of Ni layer is rather low as compared to the Co layer, leading to seriously disordered spins at the Pd/Ni interface.[30]

Ultrafast magnetization dynamics were measured by TR-MOKE to understand the influence of Pd underlayer on the magnetic damping constant. Fig. 2(a) displays the measured TR-MOKE data points measured at $H_{ex} = 11$ kOe for Pd(t_{Pd})/[Co/Ni]$_5$ samples with various t_{Pd}. All the curves exhibit a precession and damping relaxation behavior, which were fitted by using the following equation,[7,25]

$$\theta_k = a + b\exp(t/t_0) + c\sin(2\pi ft + \varphi)\exp(-t/\tau), \quad (1)$$

where the parameter a corresponds to the background signal, b and t_0 result from the slow magnetization recovery process, c, f, φ, and τ represent the precession amplitude, frequency, initial phase, and decay time of the magnetization dynamics, respectively. The fitted precession frequency f and decay time τ are respectively plotted in Fig. 2(b) and (c) as a function of H_{ex} for the cases of t_{Pd} = 5, 10, 20 nm. Apparently, the precession frequency f increases monotonically with the H_{ex}. The discrete data points are fitted with the Kittel formula, $2\pi f = \gamma(H_1H_2)^{1/2}$, where $\gamma = 18.9$ Mrad s^{-1} Oe^{-1} is the gyromagnetic ratio, $H_1 = H_{ex}\cos(\theta_H - \theta) + H_{keff}\cos^2\theta$ and $H_2 = H_{ex}\cos(\theta_H - \theta) + H_{keff}\cos 2\theta$. The magnetization equilibrium angle θ satisfies the energy-minimized equation of $\sin 2\theta = (2H_{ex}/H_{keff})\sin(\theta_H - \theta)$. As shown in Fig. 2(b), all the data points are well fitted by the solid lines, indicating that the magnetization precesses coherently in a uniform mode. The fitted effective anisotropy field H_{keff} is very close to the measured VSM data, suggesting the

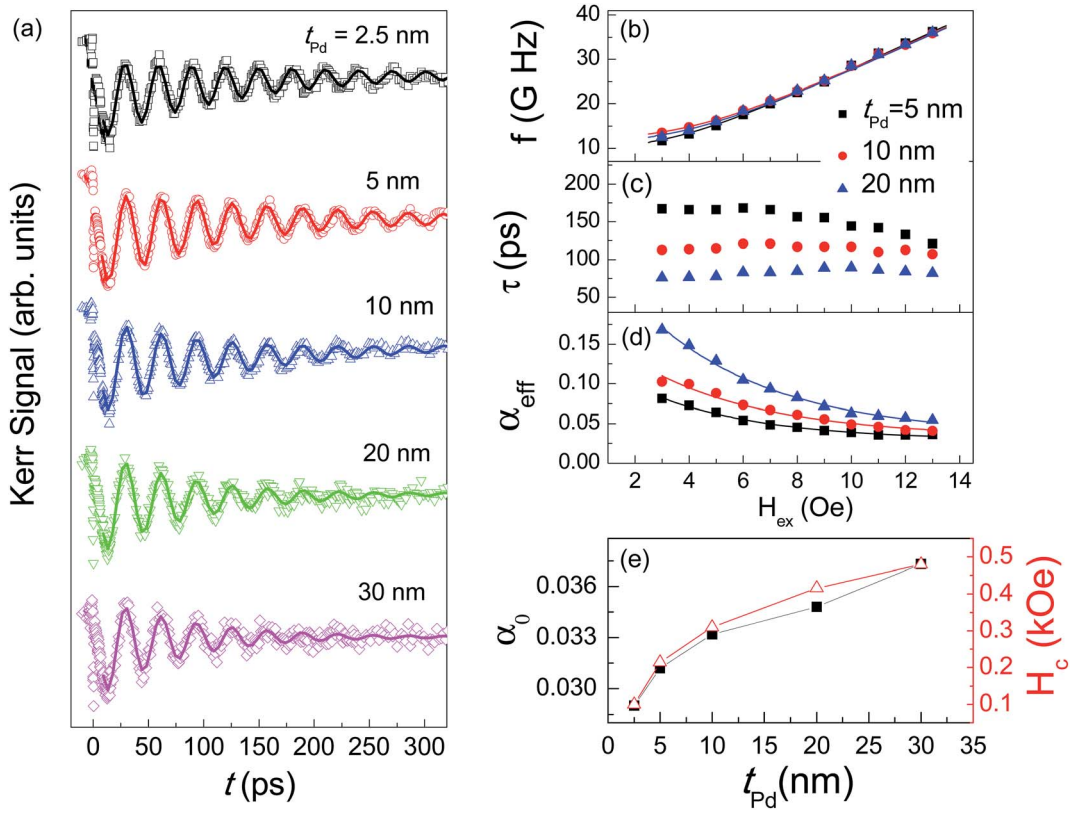

Fig. 2 (a) The laser-induced magnetization dynamic Kerr signals (open squares) and the fitting curves (solid lines) for Pd(t_{Pd})/[Co/Ni]$_5$ multilayer films with various t_{Pd} measured at the $H_{ex} = 11$ kOe and $\theta_H = 65°$. (b–d) respectively shows magnetic field dependences of precession frequency f, decay time τ, and effective Gilbert damping constant α_{eff} for t_{Pd} = 5, 10 and 20 nm. (e) The extracted magnetic damping constant α_0 and the perpendicular magnetic coercivity H_c as a function of t_{Pd}.

employed laser fluence is appropriate and the sample properties are not affected by laser pumping.

Based on the fitted f and τ, the effective damping factor α_{eff} can be derived from the simple approximate equation of $\alpha_{eff} = 1/(2\pi f\tau)$,[17,25] which includes an intrinsic damping term α_0 and an extrinsic damping term α_{ex}. It is usually believed that the extrinsic α_{ex} contains contributions from magnetic inhomogeneities, two-magnon scattering, and spin pumping effect of the adjacent nonmagnetic metal layer. The two-magnon scattering results from defects or inhomogeneities which scatter the uniform precession mode into the degenerate spin wave modes with finite wave vectors. The damping contribution due to two-magnon scattering is field angle dependent and becomes inoperative when the magnetization is oriented at an angle over 45° with the film plane. By applying a sufficiently high external magnetic field H_{ex}, the extrinsic damping terms that results from inhomogeneous distributions of magnetization and/or magnetic anisotropy can be effectively eliminated whereas the spin pumping and two-magnon scattering contributions still exist, since the field angle is 25° with respect to the film plane in our TR-MOKE measurement. As shown in Fig. 2(d), all the α_{eff} values decrease gradually with increasing the H_{ex}. Nevertheless, they are still not saturated even at the maximum applied field of H_{ex} = 13 kOe, implying the 13 kOe field is still not strong enough to completely remove the influence of magnetic inhomogeneities. In order to accurately determine the relationship between PMA strength and intrinsic magnetic damping, we utilize a decaying exponential function, $\alpha_{eff} = \alpha_{ex0}\exp(-H_{ex}/H_0) + \alpha_0$, to fit the α_{eff} data. The α_0 here corresponds to the α_{eff} value at an infinite H_{ex}, note that it still contains the extrinsic spin pumping and two-magnon scattering contributions. The fitted α_0 are displayed in Fig. 2(e) as a function of Pd layer thickness. Interestingly, distinctly different from the non-monotonic variation behavior of K_u shown in Fig. 1(c), the α_0 value keeps increasing with the increase of t_{Pd}, implying that there must be some other factors responsible for the observed increase in α_0, particularly at t_{Pd} > 10 nm where the K_u starts to decrease. The Pd layer is known to own a short spin diffusion length around 10 nm, the extra damping induced by spin pumping effect will get saturated at $t_{Pd} \sim$ 10–15 nm.[31] As we know, thicker Pd layer has a rougher surface, which gives rise to reduced exchange coupling between the interfacial magnetic atoms, as seen from the serious reduction of M_s and K_u shown in Fig. 1(c) and (d). The larger inhomogeneities and the resultant weaker exchange interaction at the Pd/FM interface, will surely enhance the two-magnon scattering effect and lead to a higher α_0 value at thicker t_{Pd} case. In order to verify our assumption, the perpendicular coercivity H_c was also measured and plotted in Fig. 2(e) for comparison. The H_c and α_0 should exhibit identical variation trends because a rough interface can not only give a thick paramagnetic dead layer, but can enhance the pinning effect of local magnetic moments as well.[19,30] As expected, the increasing tendencies of α_0 and H_c are very alike, indicating that the α_0 increase may have the same origin as H_c, *i.e.* the increased PMA strength and underlayer surface roughness.

We then measured the magnetic damping of Pd/[Ni/Co]$_5$ samples to further explore the underlying mechanism regarding the α_0 enhancement with t_{Pd}. Fig. 3(a)–(c) shows the H_{ex} dependences of precession frequency f, decay time τ, and the calculated effective damping factor α_{eff} for t_{Pd} = 5, 15 and 30 nm, respectively. Their variation behaviors are very consistent with the case of Pd/[Co/Ni]$_5$ structure, all the α_{eff} values decrease with the increase of H_{ex}, and aren't equal for different t_{Pd} at any applied field. The Pd thickness dependence of the extracted α_0 is shown in Fig. 3(d), it also increases monotonically and coincides well with the perpendicular H_c, suggesting that the results are quite consistent.

In order to clearly compare the different influences of Pd underlayer, the PMA strength K_u, the inverse of saturation magnetization ($1/M_s$) and the saturated magnetic damping α_0 are respectively shown in Fig. 4(a)–(c) for the two series samples of Ni/Co and Co/Ni. From the much higher K_u value displayed in Fig. 4(a), we know the Pd/[Co/Ni]$_5$ sample has stronger spin orbit coupling at the Pd/Co interface, which in principle should provide a larger spin pumping contribution to the magnetic damping. But on the contrary, we find that the α_0 value of Co/Ni is much lower than that of Ni/Co samples with the same Pd

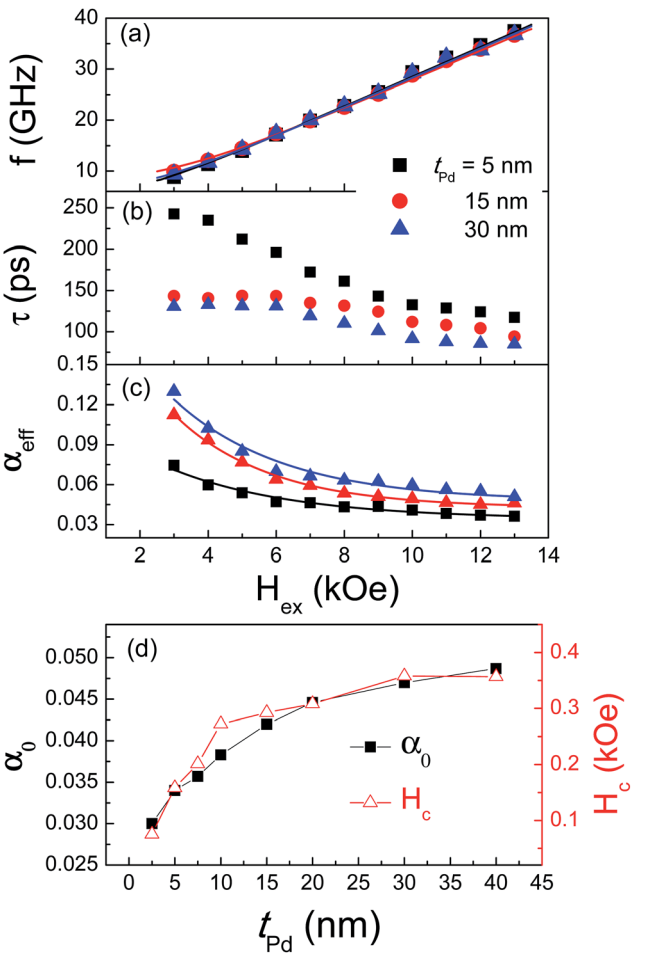

Fig. 3 (a–c) corresponds to the magnetic field dependences of magnetization precession frequency f, decay time τ, and effective Gilbert damping α_{eff} for the samples of Pd/[Ni/Co]$_5$ with t_{Pd} = 5, 15 and 30 nm. (d) The extracted damping parameter α_0 and the perpendicular magnetic coercivity H_c as a function of t_{Pd}.

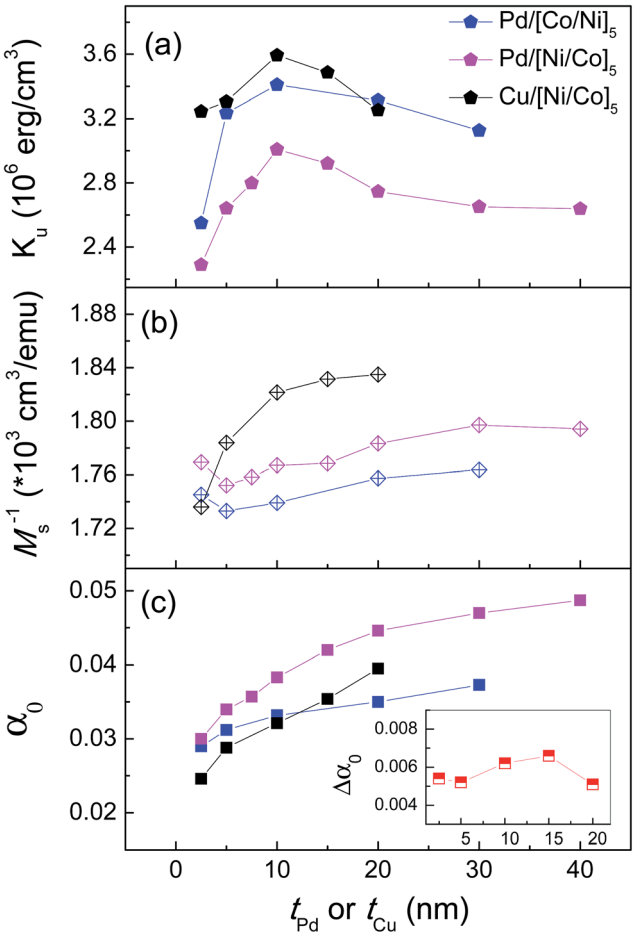

Fig. 4 The uniaxial magnetic anisotropy energy density K_u, inverse of saturation magnetization ($1/M_s$) and magnetic damping constant α_0 as a function of Pd or Cu underlayer thickness for the three types of samples. The inset of (c) shows the extra damping contribution $\Delta\alpha_0$ induced mainly by spin pumping effect of Pd layer as a function of the underlayer thickness.

thickness, again revealing that it is the weakly-exchange coupled or even decoupled interfacial spins which play an important role in the observed additional increase in α_0. The disordered spins can not only reduce the M_s, but also enhance the dissipation of spin energy *via* two-magnon scattering. In this sense, the $1/M_s$ and α_0 may follow a similar variation trend. As expected, Fig. 4(b) and (c) indicates both of them increase gradually with the Pd layer thickness, since more paramagnetic disordered spins appear at the thicker Pd/Ni or Pd/Co interface.[29,30,32] In contrast to the Co/Ni series, the Pd layer influences on the magnetic properties are more significant for Ni/Co samples, their $1/M_s$ and α_0 values are relatively larger just because the exchange interaction between Ni atoms is rather weak and magnetic spins at the Pd/Ni interface are much more disordered.

Note that for the two types of Pd-buffered multilayer samples at the thinnest Pd thickness of 2.5 nm, their α_0 values around 0.029 are the smallest and nearly equal. Nevertheless, such small value cannot be taken as the intrinsic damping constant, since the spin pumping effect of Pd layer is remarkable and not excluded. It is known the Cu layer has a quite longer spin diffusion length over 200 nm at RT, spin dephasing will not occur at the Cu thickness in a range of 0–20 nm, so the α_0 increase induced by spin pumping of Cu can be neglected.[33] As a result, in order to numerically determine the intrinsic damping and the spin pumping enhancement, we also measured and plotted the K_u and α_0 of the Cu-buffered $[Ni/Co]_5$ films in Fig. 4, with the same deposition layer sequence and sublayer thicknesses as those of Pd-buffered $[Ni/Co]_5$ samples. As shown in Fig. 4(c), although there is no spin pumping contribution for the Cu-buffered sample, the α_0 value also increases continuously with increasing t_{Cu}, owing to the increased thickness of interfacial magnetic dead layer as we discussed previously. Since the surface roughness of Cu buffer layer increases more rapidly with t_{Cu} than that of Pd buffer layer, a much faster and larger increase of $1/M_s$ for Cu-buffered $[Ni/Co]_5$ samples can be found in Fig. 4(b). The observed increasing tendency of α_0 for the Cu-buffered samples is nearly in parallel with that of Pd/$[Ni/Co]_5$. However, their difference of α_0, defined as $\Delta\alpha_0$, cannot be simply considered as the spin pumping contribution of Pd layer because the two-magnon scattering contribution of Cu is much serious than that of Pd. The inset in Fig. 4(c) shows the calculated $\Delta\alpha_0$ *versus* t_{Pd}, it increases very slightly and even drops at $t_{Pd} = 20$ nm, where the spin pumping enhancement is already saturated. This variation behavior is just because the Cu layer has a rougher surface than the Pd with the same thickness,[12] which gives a more prominent two-magnon scattering contribution. For the samples with a very thin Pd or Cu under layer, the roughness difference is not so big, so the $\Delta\alpha_0$ value of 0.0055 at $t_{Pd} = 2.5$ nm can be approximately taken as the spin pumping contribution of a 2.5 nm thick Pd layer. Accordingly, the intrinsic magnetic damping constant of our perpendicular $[Ni/Co]_5$ multilayer is estimated to be around 0.023.

Conclusion

In summary, we have studied the Pd underlayer influences on the magnetic damping, saturation magnetization and perpendicular magnetic anisotropy of $[Co/Ni]_5$ and $[Ni/Co]_5$ multilayers by time-resolved magneto-optical Kerr effect. It is found the K_u value firstly rises with t_{Pd} and then decreases after showing a maximum at $t_{Pd} = 10$ nm for both kinds of samples, owing to the competition between the roles of fcc (111) texture and magnetic dead layer at Pd/Co (or Ni) interface which are considered also responsible for the gradual reduction of M_s and monotonic increase of α_0. Interestingly, the Pd/$[Ni/Co]_5$ sample owns obviously smaller K_u and M_s but rather higher α_0, which is attributed to the presence of more disordered paramagnetic spins at Pd/Ni interface. By comparing the α_0 of Pd- and Cu-buffered $[Ni/Co]_5$ samples at $t = 2.5$ nm, the spin pumping contribution of Pd layer and intrinsic damping of perpendicular $[Ni/Co]_5$ are quantitively determined to be ~0.0055 and 0.023, respectively. These results may be helpful to understand the reported different relationships between PMA and magnetic damping, and to promise potential practical applications in high-performance SOT-memories.

Acknowledgements

This work is supported by the National Basic Research Program of China (No. 2014CB921104) and the National Natural Science Foundation of China (Grant No. 51671057, 11474067, 51222103, 11274113, 11674095 and 51201081).

References

1 S. Mangin, D. Ravelosona, J. A. Katine, M. J. Carey, B. D. Terris and E. E. Fullerton, Current-induced magnetization reversal in nanopillars with perpendicular anisotropy, *Nat. Mater.*, 2006, **5**, 210–215.

2 X. Li, Z. Zhang, Q. Y. Jin and Y. Liu, Domain nucleation mediated spin-transfer switching in magnetic nanopillars with perpendicular anisotropy, *Appl. Phys. Lett.*, 2008, **92**, 122502.

3 A. Capua, S. H. Yang, T. Phung and S. S. P. Parkin, Determination of intrinsic damping of perpendicularly magnetized ultrathin films from time-resolved precessional magnetization measurements, *Phys. Rev. B: Condens. Matter Mater. Phys.*, 2015, **92**, 224402.

4 S. Mangin, Y. Henry, D. Ravelosona, J. A. Katine and E. E. Fullerton, Reducing the critical current for spin-transfer switching of perpendicularly magnetized nanomagnets, *Appl. Phys. Lett.*, 2009, **94**, 012502.

5 H. S. Song, K. D. Lee, J. W. Sohn, S. H. Yang, S. S. P. Parkin, C. Y. You and S. Shin, Relationship between Gilbert damping and magneto-crystalline anisotropy in a Ti-buffered Co/Ni multilayer system, *Appl. Phys. Lett.*, 2013, **103**, 022406.

6 S. Pal, B. Rana, O. Hellwig, T. Thomson and A. Barman, Tunable magnetic frequency and damping in $[Co/Pd]_8$ multilayers with variable Co layer thickness, *Appl. Phys. Lett.*, 2011, **98**, 082501.

7 P. He, X. Ma, J. W. Zhang, H. B. Zhao, G. Lüpke, Z. Shi and S. M. Zhou, Quadratic Scaling of Intrinsic Gilbert Damping with Spin-Orbital Coupling in $L1_0$ FePdPt Films: Experiments and *Ab Initio* Calculations, *Phys. Rev. Lett.*, 2013, **110**, 077203.

8 S. Mizukami, E. P. Sajitha, D. Watanabe, F. Wu, T. Miyazaki, H. Naganuma, M. Oogane and Y. Ando, Gilbert damping in perpendicularly magnetized Pt/Co/Pt films investigated by all-optical pump-probe technique, *Appl. Phys. Lett.*, 2010, **96**, 152502.

9 S. Iihama, S. Mizukami, H. Naganuma, M. Oogane, Y. Ando and T. Miyazaki, Gilbert damping constants of Ta/CoFeB/MgO(Ta) thin films measured by optical detection of precessional magnetization dynamics, *Phys. Rev. B: Condens. Matter Mater. Phys.*, 2014, **89**, 174416.

10 A. Barman, S. Wang, O. Hellwig, A. Berger, E. E. Fullerton and H. Schmidt, Ultrafast magnetization dynamics in high perpendicular anisotropy $[Co/Pt]_n$ multilayers, *J. Appl. Phys.*, 2007, **101**, 09D102.

11 A. Y. Dobin and R. H. Victora, Surface Roughness Induced Extrinsic Damping in Thin Magnetic Films, *Phys. Rev. Lett.*, 2004, **92**, 257204.

12 S. Chen, M. Tang, Z. Zhang, B. Ma, S. T. Lou and Q. Y. Jin, Interfacial effect on the ferromagnetic damping of CoFeB thin films with different under-layers, *Appl. Phys. Lett.*, 2013, **103**, 032402.

13 T. Nan, S. Emori, C. T. Boone, X. Wang, T. M. Oxholm, J. G. Jones, B. M. Howe, G. J. Brown and N. X. Sun, Comparison of spin-orbit torques and spin pumping across NiFe/Pt and NiFe/Cu/Pt interfaces, *Phys. Rev. B: Condens. Matter Mater. Phys.*, 2015, **91**, 214416.

14 S. Mizukami, Y. Ando and T. Miyazaki, The Study on Ferromagnetic Resonance Line width for NM/80NiFe/NM (NM = Cu, Ta, Pd and Pt) Films, *Jpn. J. Appl. Phys.*, 2001, **40**, 580–585.

15 S. Azzawi, A. Ganguly, M. Tokaç, R. M. Rowanrobinson, J. Sinha, A. T. Hindmarch, A. Barman and D. Atkinson, Evolution of damping in ferromagnetic/nonmagnetic thin film bilayers as a function of nonmagnetic layer thickness, *Phys. Rev. B*, 2016, **93**, 054402.

16 M. H. Tang, Z. Zhang, S. Tian, J. Wang, B. Ma and Q. Y. Jin, Interfacial exchange coupling and magnetization reversal in perpendicular $[Co/Ni]_N$/TbCo composite structures, *Sci. Rep.*, 2015, **5**, 10863.

17 H. S. Song, K. D. Lee, J. W. Sohn, S. H. Yang, S. S. P. Parkin, C. Y. You and S. C. Shin, Observation of the intrinsic Gilbert damping constant in Co/Ni multilayers independent of the stack number with perpendicular anisotropy, *Appl. Phys. Lett.*, 2013, **102**, 102401.

18 D. Wu, S. Chen, Z. Zhang, B. Ma and Q. Y. Jin, Enhancement of perpendicular magnetic anisotropy in Co/Ni multilayers by *in situ* annealing the Ta/Cu under-layers, *Appl. Phys. Lett.*, 2013, **103**, 242401.

19 H. Kurt, M. Venkatesan and J. M. D. Coey, Enhanced perpendicular magnetic anisotropy in Co/Ni multilayers with a thin seed layer, *J. Appl. Phys.*, 2010, **108**, 073916.

20 A. V. D. Brink, G. Vermijs, A. Solignac, J. Koo, J. T. Kohlhepp, H. J. M. Swagten and B. Koopmans, Field-free magnetization reversal by spin-Hall effect and exchange bias, *Nat. Commun.*, 2016, **7**, 10854.

21 P. P. J. Haazen, E. Murè, J. H. Franken, R. Lavrijsen, H. J. M. Swagten and B. Koopmans, Domain wall depinning governed by the spin Hall effect, *Nat. Mater.*, 2013, **12**, 299–303.

22 L. Liu, C. F. Pai, Y. Li, H. W. Tseng, D. C. Ralph and R. A. Buhrman, Spin-Torque Switching with the Giant Spin Hall Effect of Tantalum, *Science*, 2012, **336**, 555–558.

23 K. L. Wang, J. G. Alzate and P. K. Amiri, Low-power non-volatile spintronic memory: STT-RAM and beyond, *J. Phys. D: Appl. Phys.*, 2013, **6**, 074003.

24 T. Jungwirth, J. Wunderlich and K. Olejnik, Spin Hall effect devices, *Nat. Mater.*, 2012, **11**, 382–390.

25 A. Barman and A. Haldar, Time-Domain Study of Magnetization Dynamics in Magnetic Thin Films and Micro- and Nanostructures, *Solid State Phys.*, 2014, **65**, 1–108.

26 D. Wu, W. Li, M. H. Tang, Z. Z. Zhang, S. T. Lou and Q. Y. Jin, Laser heating and oxygen partial pressure effects on the

dynamic magnetic properties of perpendicular CoFeAlO films, *J. Magn. Magn. Mater.*, 2016, **409**, 143–147.

27 E. P. Sajitha, J. Walowski, D. Watanabe, S. Mizukami, F. Wu, H. Naganuma, M. Oogane, Y. Ando and T. Miyazaki, Magnetization Dynamics in CoFeB Buffered Perpendicularly Magnetized Co/Pd Multilayer, *IEEE Trans. Magn.*, 2010, **46**, 2056–2059.

28 G. Nabiyouni and B. J. Farahani, Anomalous scaling in surface roughness evaluation of electrodeposited nanocrystalline Pt thin films, *Appl. Surf. Sci.*, 2009, **256**, 674–682.

29 S. Kim, J. Jeong, J. B. Kortright and S. Shin, Experimental observation of magnetically dead layers in Ni/Pt multilayer films, *Phys. Rev. B: Condens. Matter Mater. Phys.*, 2001, **64**, 052406.

30 J. Kim, J. W. Lee, J. R. Jeong, S. K. Kim and S. C. Shin, Influence of substrate roughness on spin reorientation transition of ultrathin Co films on Pd(111), *Appl. Phys. Lett.*, 2001, **79**, 93.

31 J. M. Shaw, H. T. Nembach and T. J. Silva, Determination of spin pumping as a source of linewidth in sputtered $Co_{90}Fe_{10}$/Pd multilayers by use of broadband ferromagnetic resonance spectroscopy, *Phys. Rev. B: Condens. Matter Mater. Phys.*, 2012, **85**, 054412.

32 N. Sato, K. P. O'Brien, K. Millard, B. Doyle and K. Oguz, Investigation of extrinsic damping caused by magnetic dead layer in Ta–CoFeB–MgO multilayers with perpendicular anisotropy, *J. Appl. Phys.*, 2016, **119**, 093902.

33 T. Gerrits, M. L. Schneider and T. J. Silva, Enhanced ferromagnetic damping in Permalloy/Cu bilayers, *J. Appl. Phys.*, 2006, **99**, 023901.